sponds to increasing values of the energy, with a unique, but important, exception concerning the AB_σ orbital. This MO belongs to subset 4, the highest in energy, but corresponds to the weakest (antibonding) metal–ligand interaction[7] and to the strongest (bonding) metal–metal coupling. The stabilization prevails, and at variance from the other MOs of subset 4, AB_σ is found rather low in energy, between subsets 1 and 2. It is unusual to notice however that two π and one δ metal–metal bonding orbitals are found *higher* in energy than their metal–metal antibonding counterparts. Table I displays the ordering of the 14 orbitals, according to EHT calculations.

According to the aufbau principle, eight electrons should be accommodated into the four MOs of the BB subset; then the AB_σ orbital should be doubly occupied, giving rise to a V–V σ bond, and the two remaining electrons should be attributed to the quasi-degenerate NB_δ and NA_{δ^*} orbitals of subset 2, thus giving rise to a probable triplet ground state. One must notice the existence of a destabilizing four-electron interaction due to the presence of both the BB_σ and the AB_σ orbitals in the doubly occupied set.

It is well-established—and the ab initio calculations on $(CpV)_2C_8H_8$ have confirmed—that the ground state of a binuclear complex can seldom be expressed in terms of a unique closed-shell configuration. If it is forced to do so, and if more than one electron pair is available for metal–metal bonding, the preferred configuration often corresponds to the localization of an even number of electrons on each metal atom, thus reducing to 0 or 1 the number of delocalized M–M bonds.[1,2,9] This is again verified for the butanediyl complex, since the ab initio SCF closed-shell configuration of lowest energy (−2577.9576 hartrees) corresponds to localizing the four metal electrons on the atomic $d_{x^2-y^2}$ orbitals, the V–V bonding AB_σ orbital being rejected into the virtual space. As in the EHT wave function, the eight remaining electrons are accommodated into the four MOs of subset 1.

Since this configuration violates Hund's rule on both metal atoms, it was expected that an open-shell quintet state in which the four metal electrons are accommodated into distinct space orbitals should lead to an improved energy value. This was corroborated by a calculation carried out on the configuration $(NB_\delta)^1\ (NA_{\delta^*})^1\ (AB_\sigma)^1\ (NA_{\sigma^*})^1$, which yielded an energy of −2578.1296 hartrees. Note that this configuration is formally nonbonding with respect to the V–V interaction, except for the minor metal–metal bonding contributions included in the underlying orbitals of subset 1.

The ground state of our complex has however little chance to be a quintet. The real nature of the ground state mainly depends upon the relative populations of orbitals AB_σ and NA_{σ^*}, knowing that an increase of the AB_σ population will enhance both the stabilization resulting from the V–V σ bond and the destabilization originating in the four-electron interaction between AB_σ and BB_σ.

The nature of the ground state was determined through CI expansions generating all singlet and all triplet configurations from the set of four singly occupied orbitals optimized in the SCF open-shell calculation carried out on the $(NB_\delta)^1\ (NA_{\delta^*})^1\ (AB_\sigma)^1\ (NA_{\sigma^*})^1$ configuration. The ground state was found to be a singlet (E_S = −2578.146 51 hartrees) corresponding to the natural orbital population $(AB_\sigma)^{1.32}\ (NB_\delta)^{1.01}\ (NA_{\delta^*})^{0.99}\ (NA_{\sigma^*})^{0.68}$. The δ and δ^* orbitals are practically equally populated. In spite of that, the lowest triplet state was found higher in energy by 926 cm^{-1} (E_T = −2578.142 29 hartrees), due to the strong coupling with configurations involving σ and σ^*. The quintet state optimized from SCF open-shell calculations is predicted to lie about 3700 cm^{-1} above the ground state. A much larger multireference SDCI expansion was also carried out, leading to minor quantitative changes with respect to these results. This CI expansion was designed to correlate eight electrons, including the BB_σ and the BB_δ electron pairs, with respect to the complete virtual space (180 MOs). The reference space included all configurations (five for the singlet state, four for the triplet) occurring with a coefficient larger than 0.06 in the small CI. The total energies obtained for the singlet and for the triplet states (respectively −2578.159 26 and −2578.154 79 hartrees) and the singlet–triplet energy separation (983 cm^{-1}) are no more than marginally affected by the account of dynamic correlation.

As for $(CpV)_2C_8H_8$,[2] the present study predicts for $(CpV)_2(C_4H_8)_2$ an antiferromagnetic V–V coupling involving four electrons, reflecting the trend toward localization of the 3d metal electrons.[9,10] As was previously done to check the electronic structure predicted for metal phthalocyanines and porphyrins,[11] we are planning to complete the present study by a joint experimental and theoretical investigation of the electron density distribution of short-bonded divanadium complexes.[12]

Acknowledgment. The calculations have been carried out on the CRAY-2 computer of the CVVR (Palaiseau, France) through a grant of computer time from the Conseil Scientifique du Centre de Calcul Vectoriel pour la Recherche.

Registry No. $(CpV)_2(C_4H_8)_2$, 104462-69-3.

---

(7) The relative strengths of the various metal–ligand interactions are illustrated by the AB_x and BB_x energy differences that can be obtained from Table I. The large splitting between the two pairs of BB_π and AB_π orbitals and the BB_δ and AB_δ orbitals indicates that the metal–ligand interaction is stronger than the metal–metal; i.e., these are mostly metal–ligand bonds. As suggested by a reviewer, the small splitting between the BB_σ and AB_σ orbitals implies that the interaction here should be interpreted as one ligand–ligand bond and one metal–metal bond. Note that the twisting of the butanediyl ligands (Figure 1) contributes to strengthening the metal–ligand stabilizing interaction in the BB_π and BB_δ MOs, but not in the BB_σ one. In this latter case, the bonding lobes of the metal orbitals are directed toward the center of symmetry of the molecule and overlap mainly with the most diffuse part of the ligand orbital combination (Figure 2).

(8) (a) Hoffmann, R. *J. Chem. Phys.* **1963**, *39*, 1397. (b) Hoffmann, R.; Lipscomb, W. N. *J. Chem. Phys.* **1962**, *36*, 2179, 3489; *37*, 2872. EHT parameters for vanadium are taken from: Kubacek, P.; Hoffmann, R.; Havlas, Z. *Organometallics* **1982**, *1*, 180.

(9) (a) Garner, C. D.; Hillier, I. H.; Guest, M. F.; Green, J. C.; Coleman, A. W. *Chem. Phys. Lett.* **1976**, *41*, 91. (b) Bénard, M.; Veillard, A. *Nouv. J. Chim.* **1977**, *1*, 97. (c) Guest, M. F.; Hillier, I. H.; Garner, C. D. *Chem. Phys. Lett.* **1977**, *48*, 587. (d) Bénard, M. *J. Chem. Phys.* **1979**, *71*, 2546. (e) Wiest, R.; Bénard, M. *Theoret. Chim. Acta* **1984**, *66*, 65. (f) Noodleman, L. *J. Chem. Phys.* **1981**, *74*, 5737.

(10) (a) Bénard, M. *Theoret. Chim. Acta* **1982**, *61*, 379. (b) Bénard, M. *Chem. Phys. Lett.* **1983**, *96*, 183. (c) Newton, M. D. *Chem. Phys. Lett.* **1982**, *90*, 291. (d) Messmer, R. P.; Caves, T. C.; Kao, C. M. *Chem. Phys. Lett.* **1982**, *90*, 296.

(11) (a) Li, N.; Coppens, P.; Landrum, J. *Inorg. Chem.* **1988**, *27*, 482 and references therein. (b) Bénard, M. *Angew Chem., Int. Ed. Engl.* **1982**, *21*, 868. (c) Rohmer, M.-M. *Inorg. Chem.* **1989**, *28*, 4574.

(12) Krüger, C.; Goddard, R.; Poumgba, C.; Daniel, C.; Bo, C.; Bénard, M. Work in progress.

Contribution from the School of Chemical Sciences,
University of East Anglia, Norwich NR4 7TJ, England,
and Institut Laué-Langevin, Grenoble 38042, France

Valence Localization in Triangular Trimanganese(II,2III) Complexes[1]

Ladda Meesuk, Ross P. White, Barry Templeton,
Upali A. Jayasooriya, and Roderick D. Cannon*

Received August 29, 1989

Mixed-valence trinuclear complexes of the general type $[M^{III}_2M^{II}O(OOCR)_6L_3]$ (Figure 1) are expected to show either trigonal or lower symmetry depending on the rate of intramolecular electron transfer in relation to the time scale of the measurement. For most complexes of this class, X-ray crystallography indicates

---

* To whom correspondence should be addressed at the University of East Anglia.

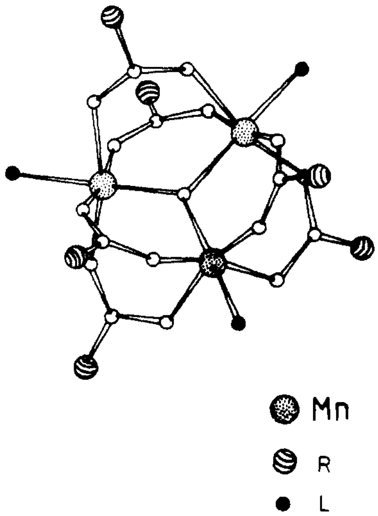

Figure 1. Molecular structure of the complexes $[Mn_3O(OOCR)_6L_3]^{n+}$.

trigonal symmetry,[2] but for several triiron(II,2III) complexes, infrared data point conclusively to the lower symmetry.[3,4] In other words, the ground state ($2Fe^{3+} + Fe^{2+}$) is localized by vibronic distortions such as the lengthening of Fe^{II}–O and shortening of Fe^{III}–O bonds, though not excluding some mixing with the electronically excited configuration ($2Fe^{2.5+} + Fe^{3+}$). In addition, however, there can be a thermally activated electron-transfer process, which amounts to a small polaron hopping between adjacent ions in the Fe_3 triangle:

$$Fe^{III}Fe^{III}Fe^{II} \rightarrow Fe^{III}Fe^{II}Fe^{III} \qquad (1)$$

An example of such behavior in the solid state is the compound $[Fe^{III}_2Fe^{II}O(OOCCH_3)_6(py)_3](py)$ (**1**), for which additional data including Mössbauer spectroscopy and specific heat measurements imply a combination of static and dynamic rotational disorder.[5] Also in solution, at room temperature, complexes such as $[Fe^{III}_2Fe^{II}O(OOCCMe_3)_6(py)_3]$ are localized on the IR time scale but appear delocalized on the NMR time scale.[4]

It seems possible that complexes of some other metals will behave in the same way, while others again may adopt a fully delocalized $(M^{2.67+})_3$ configuration with no hopping process. So far, there are no kinetic data on any system other than the iron complexes, but one particularly interesting comparison is the pair of mixed-valence complexes $[Mn_3O(OOCCH_3)_6L_3](L)$, with L = C_5H_5N (**2**) and L = $3\text{-}ClC_5H_4N$ (**3**). X-ray studies indicate that **2** has rigorous 3-fold symmetry, with the noncoordinated pyridine molecules rotationally disordered on the C_3 axes,[6,7] while **3** has nonequivalent metal atoms and bond distances characteristic of Mn^{III} and Mn^{II}.[8] However we now report infrared data which show that both of these mixed-valence complexes have the lower symmetry, indicating valence localization. Our approach is based on comparisons with the analogous fully oxidized $[Mn_3O(OOCCH_3)_6(py)_3]^+$ species and with previously documented oxidized and mixed-valence iron complexes.[9-13]

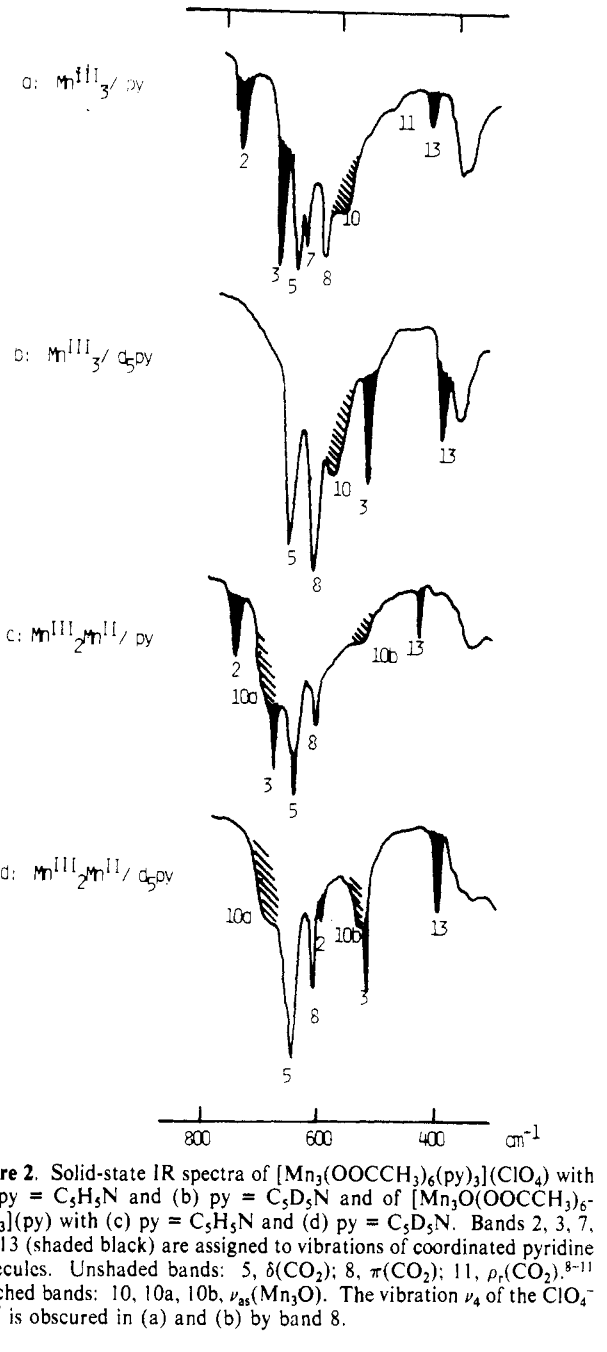

Figure 2. Solid-state IR spectra of $[Mn_3(OOCCH_3)_6(py)_3](ClO_4)$ with (a) py = C_5H_5N and (b) py = C_5D_5N and of $[Mn_3O(OOCCH_3)_6(py)_3](py)$ with (c) py = C_5H_5N and (d) py = C_5D_5N. Bands 2, 3, 7, and 13 (shaded black) are assigned to vibrations of coordinated pyridine molecules. Unshaded bands: 5, $\delta(CO_2)$; 8, $\pi(CO_2)$; 11, $\rho_r(CO_2)$.[8-11] Hatched bands: 10, 10a, 10b, $\nu_{as}(Mn_3O)$. The vibration ν_4 of the ClO_4^- ion[27] is obscured in (a) and (b) by band 8.

The salt $[Mn_3O(OOCCH_3)_6(py)_3]ClO_4$ (**4**) has been prepared previously,[9,14,15] and a detailed analysis of the IR spectrum supports the oxo-centered trinuclear structure.[9] It has been described as dark brown or black in color, but we find that the purest products, obtained by rapid crystallization from reaction mixtures in acetic acid, with high perchloric acid and low pyridine concentrations, are a sandy ocher color. Nonacidic solvents such as ethanol, and

---

(1) Vibrational Spectra of Carboxylate Complexes. 8. Parts 3, 5–7: Refs 9–12.

(2) Cannon, R. D.; White, R. P. *Prog. Inorg. Chem.* **1988**, *36*, 195.

(3) Meesuk, L.; Jayasooriya, U. A.; Cannon, R. D. *J. Am. Chem. Soc.* **1987**, *109*, 2009.

(4) White, R. P.; Wilson, L. M.; Williamson, D. J.; Moore, G. R.; Jayasooriya, U. A.; Cannon, R. D. *Spectrochim. Acta*, in press.

(5) Sorai, M.; Kaji, K.; Hendrickson, D. N.; Oh, S. M. *J. Am. Chem. Soc.* **1986**, *108*, 702.

(6) Vincent, J. B.; Chang, H.-R.; Folting, K.; Huffman, J. C.; Christou, G.; Hendrickson, D. N. *J. Am. Chem. Soc.* **1987**, *109*, 5703.

(7) Jang, H. G.; Vincent, J. B.; Nakano, M.; Huffman, J. C.; Christou, G.; Sorai, M.; Wittebort, R. J.; Hendrickson, D. N. *J. Am. Chem. Soc.* **1989**, *111*, 7778.

(8) Baikie, A. R. E.; Hursthouse, M. B.; New, L.; Thornton, P.; White, R. G. *J. Chem. Soc., Chem. Commun.* **1980**, 684. See further: Oh, M. H.; Hendrickson, D. N.; Hassett, K. L.; Davis, R. E. *J. Am. Chem. Soc.* **1985**, *107*, 8009.

(9) Johnson, M. K.; Powell, D. B.; Cannon, R. D. *Spectrochim. Acta* **1981**, *37A*, 995.

(10) Montri, L.; Cannon, R. D. *Spectrochim. Acta* **1985**, *41A*, 643.

(11) Meesuk, L.; Jayasooriya, U. A.; Cannon, R. D. *Spectrochim. Acta* **1987**, *43A*, 687.

(12) Cannon, R. D.; Montri, L.; Brown, D. B.; Marshall, K. M.; Elliott, C. M. *J. Am. Chem. Soc.* **1984**, *106*, 2591.

(13) White, R. P.; Chaisa-ard, N.; Bollen, S. K.; Cannon, R. D.; Jayasooriya, U. A.; Robertson, S. T.; Steigenberger, U.; Tomkinson, J. *Spectrochim. Acta*, in press.

(14) Uemura, S.; Spencer, A.; Wilkinson, G. *J. Chem. Soc., Dalton Trans.* **1973**, 2565.

(15) Vincent, J. B.; Christmas, C.; Huffman, J. C.; Christou, G.; Chang, H.-R.; Hendrickson, D. N. *J. Chem. Soc., Chem. Commun.* **1987**, 236.

higher pyridine concentrations, favor the mixed-valence product, which is black.[16] The mixed-valence compound can be obtained with variable stoichiometry, $[Mn_3O(OOCCH_3)_6L_3](L)_x$, the pyridine being easily removed by pumping. IR spectra were not significantly affected down to $x = 0.2$, but the samples used here had $x = 1.0$. With more bulky ligands such as 4-methylpyridine and 3-chloropyridine, values of x close to 0.5 were usual. The oxidized compounds have no noncoordinated organic base.

Experimental Section

$[Mn_3O(OOCCH_3)_6(py)_3]ClO_4$. "Manganic acetate", $Mn(OAc)_3 \cdot 2H_2O$ (2.7 g, 0.01 mol), prepared from $Mn(OAc)_2$ and $KMnO_4$,[18] was dissolved in a mixture of ethanol (20 mL) and acetic acid (4 mL) and the mixture was warmed to 45 °C with stirring to give a brown solution. Anhydrous $NaClO_4$ (1.2 g, 0.01 mol) dissolved in warm pyridine (4 mL) was added. After the mixture was stirred at 45 °C for 2 min and allowed to cool, fine golden brown needles were filtered off in air, washed with ethanol and with diethyl ether, and dried over P_2O_5. Yield: 2.5 g (86%). Anal. Calcd for $C_{27}H_{33}ClMn_3N_3O_{17}$: C, 37.20; H, 3.82; N, 4.82; Cl, 4.07; Mn, 18.9. Found: C, 36.44; H, 3.57; N, 4.43; Cl, 4.36; Mn(III), 18.53; Mn(total), 18.93.

$[Mn_3O(OOCCH_3)_6(py)_3](py)$. In a nitrogen-filled Schlenk tube, "manganic acetate" (5.4 g, 0.02 mol) was dissolved in warm pyridine (20 mL, 70 °C) to form a black solution. Heating was continued for 5 min at 70 °C. After the solution was cooled to room temperature and allowed to stand for 48 h, shiny black crystals were filtered off in the open air and dried over CaO. The product is reasonably stable to air oxidation. Yield: 1.5 g, 27%. Anal. Calcd for $C_{32}H_{38}Mn_3N_4O_{13}$: C, 45.14; H, 4.50; N, 6.58; Mn(III), 12.90; Mn(total), 19.36. Found: C, 44.58; H, 4.48; N, 6.42; Mn(III), 12.97; Mn(total), 19.55.

$[Mn_3O(OOCCH_3)_6(3\text{-}ClC_5H_4N)_3](3\text{-}ClC_5H_4N)_x$. This was prepared as above by using 0.14 g of manganic acetate and 0.5 mL of 3-chloropyridine. Anal. Calcd for $x = 0.5$: C, 37.96; H, 3.43; N, 5.25; Cl, 13.32. Found: C, 37.25; H, 3.28; N, 5.24; Cl, 13.72.

Manganese(III) content was determined by treating the solid sample with excess iron(II) in dilute sulfuric acid and back-titrating with cerium(IV). Total manganese content was determined by reducing to manganese(II) with aqueous hydroxylammonium chloride and titrating with $Na_2H_2(edta)$ using pyrocatechol violet indicator.

Results and Discussion

Parts a and b of Figure 2 show spectra of $[Mn_3O(OOCCH_3)_6(py)_3]ClO_4$ (**4**) and of the perdeuteriopyridine analogue. Bands are assigned and numbered by comparison with previous work on this and the corresponding Cr_3O and Fe_3O complexes.[9,10] After vibrations of pyridine, acetate, and ionic perchlorate are accounted for, as detailed in the caption, one broad band (band 10) is assigned to $\nu_{as}(Mn_3O)$, the doubly degenerate in-plane vibration of the central oxygen. Parts c and d of Figure 2 show spectra of the mixed-valence compound $[Mn_3O(OOCCH_3)_6(py)_3](py)$ (**2**) and the perdeuteriopyridine analogue. Assignments of pyridine and carboxylate modes are made by comparison with **4** and with mixed-metal and mixed-valence iron analogues.[11,12] They leave two bands, 10a,b, assigned to $\nu_{as}(Mn_3O)$, showing that this mode is split by lowering of symmetry from D_{3h} to C_{2v}. The spectrum of the 3-chloropyridine adduct **3** is more complicated (Figure 3), but the additional bands, relative to Figure 2, are assigned to the substituted pyridine by a comparison with the spectrum of the free base. The two components of $\nu_{as}(Mn_3O)$ are at similar frequencies in the two compounds **2** and **3**.

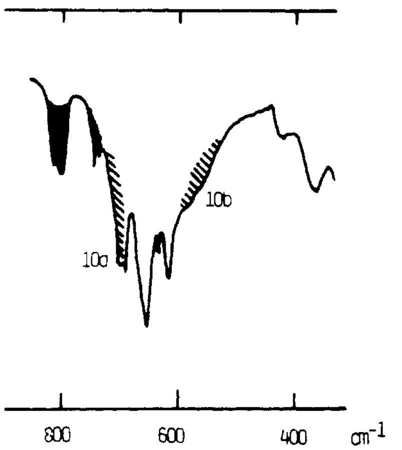

Figure 3. Infrared spectrum of $[Mn_3(OOCCH_3)_6(NC_5H_4Cl\text{-}3)_3](NC_5H_4Cl\text{-}3)_{0.5}$. The shading and numbering of bands correspond to Figure 2.

We propose that on the time scale of vibrational motion, both mixed-valence compounds have a comparable degree of valence trapping, in spite of the fact that the pyridine adduct has crystallographic trigonal symmetry while the chloropyridine adduct has a lower symmetry. The pyridine adduct **2** undergoes a first-order phase transition at 184.7 K,[6,7] above which the noncoordinated pyridine molecules begin complicated motions. The iron complex **1** has a second-order transition in the range ca. 115–190 K, associated with the onset of pyridine rotation and electron transfer.[5] What the IR data show is that, even up to 300 K, valences in individual trimer molecules remain to some extent localized, so that electron transfer can still be considered to be thermally activated.

As is well-known, the structural and redox chemistries of iron(III) and manganese(III) are in general very different; hence it is somewhat remarkable to find a pair of complexes such as **1** and **2** behaving so similarly. Moreover, the magnetic properties of these particular compounds also differ significantly, and in such a way as might have suggested that while the triiron(II,2III) complex is localized, the trimanganese(II,2III) complex would be delocalized, either completely, or at least to a greater extent than the iron complex. For the iron complex, antiferromagnetic coupling constants $J(Fe^{III}\text{–}Fe^{III})$ and $J(Fe^{III}\text{–}Fe^{II})$ have been determined spectroscopically as −60 and −18 cm^{-1}, respectively.[19] For the manganese complex, bulk magnetic susceptibility measurements[6] give much smaller values, $J(Mn^{III}\text{–}Mn^{III})$ and $J(Mn^{III}\text{–}Mn^{II}) = -8.3$ and -5.1 cm^{-1}. The preferred mechanism of coupling is superexchange via the central oxide ion.[20] On the other hand, valence delocalization is promoted by high (negative) values of the electron tunneling integral (b, W_S, and β in the notations of ref 21). Theoretical treatments indicate that high negative values of J tend to frustrate the effects of tunneling, i.e. to favor localization of valence, other factors such as metal–ligand geometry and force constants being equal.[22-25] Thus it is

---

(16) Both the oxidized and the mixed-valence manganese compounds were first obtained by Weinland and Fischer.[17] They reported a series of perchlorate and nitrate salts, variously colored "umber brown" and "light umber brown", and other products with no inorganic anion, dark brown and soluble in organic solvents.

(17) Weinland, R. F.; Fischer, G. *Z. Anorg. Allg. Chem.* **1921**, *120*, 161.

(18) Brauer, G. *Handbook of Preparative Inorganic Chemistry*; Academic Press: London, 1965; Vol. 2, p 1469. While this work was in progress, Christou, Hendrickson, and co-workers reported a preparative method using the organic-soluble $[n\text{-}Bu_4N]MnO_4$ in place of $KMnO_4$ as oxidant.[6,15]

(19) White, R. P.; Al-Basseet, J. O.; Cannon, R. D.; Kearley, G. J.; Jayasooriya, U. A. *Physica B* **1989**, *156, 157*, 367.

(20) Blake, A. B.; Yavari, A.; Hatfield, W. E.; Sethulekshmi, C. N. *J. Chem. Soc., Dalton Trans.* **1985**, 2509.

(21) (a) Launay, J. P.; Babonneau, F. *Chem. Phys.* **1982**, *67*, 295. (b) Borshch, S. A.; Kotov, I. N.; Bersuker, I. B. *Chem. Phys. Lett.* **1982**, *89*, 381. (c) Cannon, R. D.; Montri, L.; Brown, D. B.; Marshall, K. M.; Elliott, C. M. *J. Am. Chem. Soc.* **1984**, *106*, 2591.

(22) Cox, P. A. *Chem. Phys. Lett.* **1980**, *69*, 340.

(23) (a) Belinskii, M. I.; Tsukerblat, B. S.; Gerbeleu, N. V. *Fiz. Tverd. Tela (Leningrad)* **1983**, *25*, 869; *Sov. Phys.—Solid State (Engl. Transl.)* **1983**, *25*, 497. (b) Tsukerblat, B. S.; Belinskii, M. I. *Fiz. Tverd. Tela (Leningrad)* **1983**, *25*, 3512; *Sov. Phys.—Solid State (Engl. Transl.)* **1983**, *25*, 2024. (c) Belinskii, M. I.; Tsukerblat, B. S. *Fiz. Tverd. Tela (Leningrad)* **1984**, *26*, 758; *Sov. Phys.—Solid State (Engl. Transl.)* **1984**, *26*, 458.

somewhat surprising that the manganese system should resemble the iron system so closely.[26] It suggests that other mixed-valence systems[2] which have rather low *J* values, such as ($Cr^{III}{}_2Cr^{II}$) and ($V^{III}{}_2V^{II}$), may also show thermally activated electron hopping.

Acknowledgment. This research was supported by the Science and Engineering Research Council, with a studentship to R.P.W., and by the University of East Anglia and the ORS, with scholarships to L.M.

---

(24) (a) Borshch, S. A.; Kotov, I. N.; Bersuker, I. B. *Teor. Eksp. Khim.* **1984**, *20*, 675; *Theor. Exp. Chem.* (*Engl. Transl.*) **1984**, *20*, 633. (b) *Chem. Phys. Lett.* **1984**, *111*, 264. (c) *Khim. Fiz.* **1984**, *3*, 667; *Sov. J. Chem. Phys.* **1985**, *3*, 1009.

(25) Belinskii, M. I. *Fiz. Tverd. Tela* (*Leningrad*) **1985**, *22*, 1761; *Sov. Phys.—Solid State* (*Engl. Transl.*) **1985**, *27*, 1057.

(26) A reviewer commented that localization of valency in the trimanganese(II,2III) case is "not too surprising" in view of the earlier triiron(II,2III) data and in view of the "fact that the intramolecular magnetic exchange interactions (related to tunneling matrix elements) are smaller in the Mn_3O complexes than in the Fe_3O complexes". We are not aware that the two types of interaction are related, and as stated in the text, they actually affect the electronic structure in opposite ways. Although surprise can only be a subjective response to the data, we agree rather with the authors of ref 6, that, given present knowledge, the behavior of the manganese complexes can be considered surprising rather than unsurprising. Another reviewer points out that, in trimanganese(II,2III), the electron transfers between e_g orbitals, whereas in triiron(II,2III) it transfers between t_{2g} orbitals. This increases the vibronic energy barrier in the manganese case; in fact, it also accounts for many of the characteristic differences between manganese and iron chemistry noted in the text.

(27) Siebert, H. *Z. Anorg. Allg. Chem.* **1954**, *275*, 225.